Nonlinear Static Stiffness of Rail Pads for Different Materials and Thicknesses using Finite Element Method

Arif Khuarizmi Mazlan, Abdul Malek Abdul Wahab[*],
Muhamad Azhan Anuar, Ahmad Khushairy Makhtar
School of Mechanical Engineering, College of Engineering,
Universiti Teknologi MARA, 40450 Shah Alam, Selangor, Malaysia
[*]abdmalek@uitm.edu.my

ABSTRACT

The rail pad located in between the steel rail and base plate provides flexibility to the track and cushions from shocks and vibrations resulting from train operation. This polymeric material has nonlinear behaviour. In this study, the behaviour of the rail pad for different polymeric materials and various thicknesses was investigated. The three different types of rail pads were ethylene propylene diene monomer (EPDM), thermoplastic elastomers (TPEs) and ethylene vinyl acetate (EVA). Three-dimensional (3D) finite element (FE) approach was used to model the fastening system under the static load. The Abaqus software was used for the FE analysis. The thicker rail pad deformed more than the thinner for the same load value. Comparing the thickness, EPDM pad had the highest amount of deformation which had an average difference of 40%, *followed by TPE and then EVA with* 33% and 23% respectively. *The static stiffness of EVA material was the highest followed by TPE and EPDM. For all materials, the rail pad became stiffer as thickness decreased. The reaction force decreased as the thickness of the rail pad increased. EVA, TPE and EPDM showed 15%, 9% and 5% reduction of reaction force respectively as the rail pad thickness increased from 5 mm to 10 mm. Despite that, in term of material, EVA had highest capability to reduce reaction force compared to EPDM and TPE.*

Keywords: *Rail Track System; Baseplate Fastening; Deflection Rail; Rail Pad and Nonlinear Curve*

Introduction

As the number of people who use rail as their major form of transportation grows, maintaining the greatest quality of service and safety is essential in the rail industry. The rail fastening system is one of the important parts that allows the railway system to function properly [1]. The reliability of the track fastening system is crucial for sustainable life cycle strategy and effective protection against vibration and structure-borne noise [2]. The rail pad which is placed beneath the rail is an integral part of the fastening mechanism [3]–[5]. The existence of rail pads in the system gives the flexibility to the track and dampens the forces of vibration [3], [6]. Rail pad stiffness has a great influence on track operation for slab track. The changes in track stiffness creates an interaction force where the degradation of track arises due to the permanent deformation of the ballast [7]-[8]. Track degradation is one of the many causes of accidents which can harm people inside the train. This issue is not only due to the safety aspects but is also related to high-cost maintenance issues.

The behaviour of the polymeric rail pad has attracted the interest of numerous scholars. Experimental and numerical computation has been carried out to investigate the condition of the rail pad. Experimental work by Wei et al. stated that the vertical stiffness of TPE rail pads is directly proportional to the load amplitude [9]. The stiffness of the rail pad increased with load frequency, in experiments by Zhu et al. [10] and Wei et al. [11]. On the other hand, other researchers have used numerical approaches to anticipate the behaviour of nonlinear mechanical rail pads [12]. The rail, sleeper, rail pad, rail clip, shoulder and insulator had all been included in Zhang et al.'s [1] finite element (FE) model of the fastening system. They investigated the impact of preload on the performance of fastening systems. Koroma et al. [13] used FE to model the rail pad under static and dynamic loads, claiming that the nonlinearity of the rail pad and preload influenced track vibration.

In this study, the focus was on the behaviour of the rail pad under static loads by using a three-dimensional (3D) FE approach. Three different types of rail pads (i.e., ethylene propylene diene monomer (EPDM), thermoplastic elastomers (TPEs) and ethylene vinyl acetate (EVA)) with various thicknesses were investigated. The static stiffness and force reaction were predicted and analysed.

The laboratory and field investigation were constrained in terms of time and cost for design solutions. As a result, the finite element method (FEM) was created to do a quick study of crucial variables' effects. The generated model can be used to predict the behaviour of rail pad in static condition under various parametric conditions. This method can be utilised as a decision-making aid for proactive measures in rail operation.

3D modelling of rail fastening system

Figure 1 shows the rail, rail pad and baseplate which had been used in this study. All the three components had been assembled as shown in Figure 2 and had been analyzed using ABAQUS software.
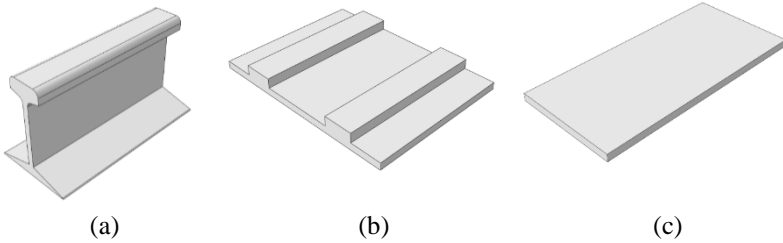

(a)   (b)   (c)

Figure 1: Isometric view of: a) rail UIC 60; b) cast iron baseplate;
c) rail pad

Materials properties

The steel rail and cast-iron baseplate were designed using a 3D deformable solid element with the extrusion type of base feature. The solid materials such as steel and cast iron had been assigned as elastic materials as reported in the previous experimental studies [14].

The rail pad had been modelled using 3D deformable solid element with the extrusion type of base feature. The rail pad had been made from rubber type materials. Thus, the materials properties of rail pad were assigned as hyper-elastic which showed the nonlinearity behaviour. The neo-Hookean (NH) was applied for modelling the hyperelastic material. The NH model depended on two material parameters which were bulk modulus, κ, and shear modulus, μ for determining the compressible and incompressible deformation conditions. Equation (1) shows the compression model for NH in terms of Cauchy stress equation.

$$\sigma = \frac{\mu}{J} dev[b^*] + \kappa(J - 1)$$

(1)

where J is a Jacobian determinant, b is a left Cauchy–Green deformation tensor and I is a unity tensor. In this study, three different materials of EPDM, TPE and EVA, which have been commonly used in the railway line industry, were modelled. Table 1 shows the material properties of the rail pad, steel rail and cast-iron plate. The specifications and dimensions of the components had been based on previous research papers [1], [14]-[15].

Table 1 Basic properties of steel rail, cast iron base plate and rail pad

	Density, ρ (kg m^{-3})	Coefficient of Thermal Expansion, α C^{-1}	Young's Modulus, E MPa	Poisson's Ratio, v	Tensile Yield Strength, σ MPa	Tensile Ultimate Strength, σ MPa	Initial Shear Modulus Mu, GPa	Incompressibility Parameter D1, K Pa^{-}
EPDM	2000	0.000165	11.2	0.43	5.5	25	3916000	7.5^{-8}
TPE	1300	0.00013	30	0.41	34.5	52	10638000	3.6^{-8}
EVA	940	0.00016	40	0.49	30	40	13423000	3^{-9}
Type of track structure	Density, ρ (kgm^{-3})	Coefficient of Thermal Expansion, α C^{-1}	Young's Modulus, E MPa	Poisson's Ratio, v	Tensile Yield Strength, σ MPa	Compressive Yield Strength, σ MPa	Tensile Ultimate Strength, σ MPa	Compressive Ultimate Strength, σ MPa
Structural Steel (rail)	7850	0.000012	200000	0.3	250	250	460	172
Concrete (sleeper)	2300	0.000014	30000	0.18	5	40	5	41

Load, boundary conditions and meshing

Figure 2 shows the load and boundary conditions which had been applied to the rail fastening model. The static vertical load was applied uniformly on the rail head to demonstrate the force from the wheels. The static compression loads were applied in the range of 10-90 kN and preloaded at 10 kN as the toe load [14]. The deformation of the rail pad was computed. The fixed support was applied on the bottom surface of the baseplate.

The interaction between different materials was considered due to three parts being in contact with each other to develop the fastening system model. The interactions between the component tracks were formulated by using the surface-to-surface contact. In this work, two in-contact surfaces occurred on the pad-frame and pad-rail. For each of the contact pairs, master and slave surface was defined. This was to prevent any large and undetected penetrations from occurring. The contacting bodies had been pressured as shown by the coefficient of friction (COF) which interacted with the maximum allowable frictional stress [1]. The value of COF was 0.3 as based on literature [15]. In the normal behaviour of contact property, hard contact was considered between the other components. It allowed the separation of components and transfer of compressive normal forces while neglecting the tensile normal forces [13]-[14].

For the meshing, all the components were set in 3D linear hexahedral solid element. The 3D hexahedral solid element consisted of eight nodes and each nodes had three translational degrees of freedom [15]. The suitable size of the mesh was decided based on a mesh convergence test. The large size of meshing caused inaccurate simulation results. Higher refinement of meshing increased the computing time. Thus, suitable size of mesh needed to be applied to ensure accurate simulation results were produced within the optimum time.
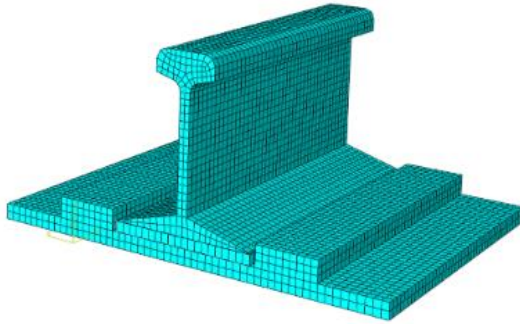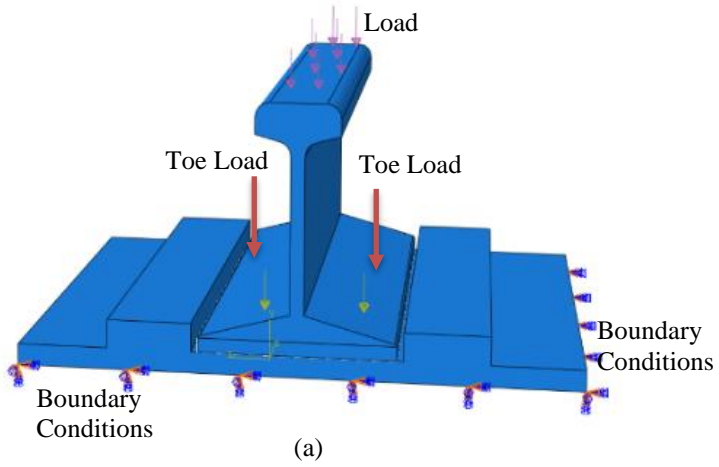
(a)

(b)

Figure 2: (a) Loads applied and boundary condition (b) meshing of the fastening system

Results and Discussion

Validation of simulation

Table 2 shows the study's mesh configuration settings. As shown in the table, deformation was inversely related to element count. The total deformation fluctuated as the number of parts dropped until at 1.28 mm. The simulations with 13889 elements produced results that were comparable with finding by [18]. Thus, in the current investigation, 13889 elements were used for additional simulation.

Table 2: Mesh setting parameters

| Element Size (mm)	Nodes	Elements	Total Deformation at 90 KN (mm)
5	46055	33660	1.20
6	31314	22500	1.22
7	20548	13889	1.28
8	15132	10032	1.54
9	9884	4114	1.58
10	8132	3832	1.66
11	6084	3600	1.71

The validation was performed with experimental data from a previous research paper [18]. In the experimental work, a universal servo-hydraulic testing device with a load cell with a capacity of under 100 kN was used to conduct stiffness tests. Four LVDTs (Linear Variable Differential Transformers) were used to measure the deformation of the rail pads. The vertical load and rail pad deformation were measured during the stiffness testing, with the latter being the average of the four LVDTs.

Similar geometry, materials properties, boundary conditions and load of the rail pad were applied in the simulation. Figure 3a shows the simulation results of the deformation of the EPDM rail pad. Figure 3b shows the comparison between the simulation and previous experimental work for EPDM rail pad of load versus deformation. The simulation results were in good agreement with the experimental data.

The percentage error between simulation and previous experimental data was tabulated in Table 3. The higher percentage errors at loads 10 kN and 20 kN were due to rigid body displacement, which is a common problem for geometrically nonlinear small-strain condition [19]. This problem could been neglected since the average value of percentage error was 6.5% which was considered as an acceptable range to verify the accuracy of the model simulation. Additionally, the rigid body displacement occurred at a very small value compared to other deformations.
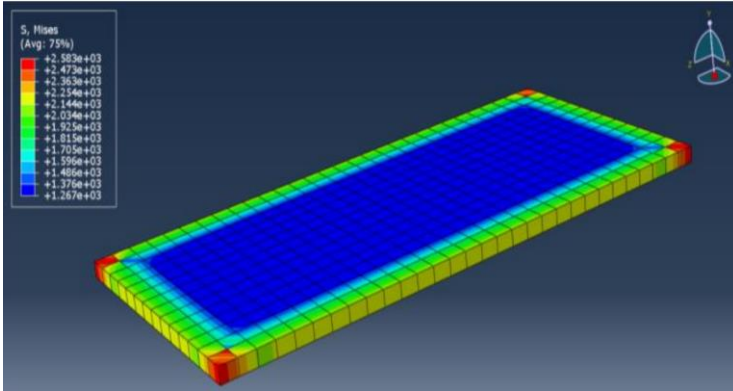
(a)
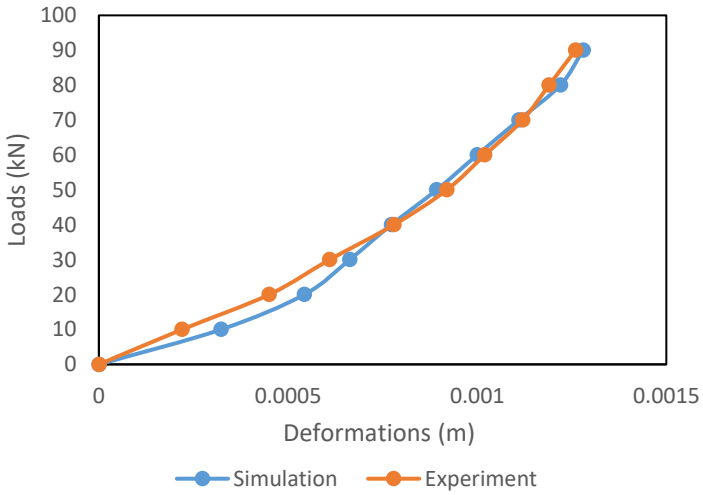
(b)

Figure 3: EPDM rail pad deformation (a) simulation results
(b) comparison between simulation and experimental results [18]

Table 3: Percentage error for reference and simulation results

Load (KN)	Deformation (mm)		Percentage error (%)
	Reference	Simulation	
0	0.00	0.00	0.00
10	0.22	0.32	31.25
20	0.45	0.54	16.67
30	0.61	0.66	7.50
40	0.78	0.77	1.29
50	0.92	0.89	3.37
60	1.02	1.00	2.00
70	1.12	1.11	0.90
80	1.19	1.22	2.45
90	1.26	1.28	1.59

Rail pad thickness

Figure 4 shows the effects of the material for the rail pad under the static compression loads for three different types of rail pads. The rail pad thickness was between 4.0–10 mm. Due to the hyperelastic material behaviour, the deformation of the rail pad increased non-linearly in the presence of reaction force exerted on the rail. The results showed that the EPDM pad had the highest amount of deformation followed by TPE and EVA for all the thicknesses. This result was in line with [18].

In general, the deformation of the rail pad was related to the elasticity modulus. The deformation of the rail pad was shown to be inversely proportional to the value of the elasticity modulus [20]. Table 1 shows that the modulus elasticity for EPDM was the lowest followed by TPE and EVA. Thus, it was evident that EPDM had the highest deformation followed by TPE and EVA when comparing between the rail pad materials.

In term of thickness, the modulus elasticity values decreased as thickness increased [21]. Figure 5 shows the larger deformation occurred at thicker rail pad for all materials. Comparing 10 mm and 4 mm thickness of the rail pad, it could be seen that in all cases, for the same load value, the thinner rail pad involved fewer displacements than the thicker one. The rail pad in which this effect was greatest was the EPDM, which had an average difference of 40%. The other two rail pads behaved in a similar way, 33% in the case of TPE and 23% in the case of EVA. This trend was in agreement with the results reported by Amjadi and Fatemi [20].
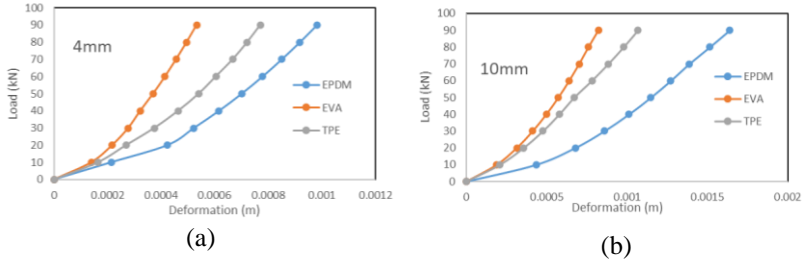
(a)

(b)

Figure 4: The deformation graph of three different types of material rail pads for various thicknesses and loads

(a)

(b)

(c)
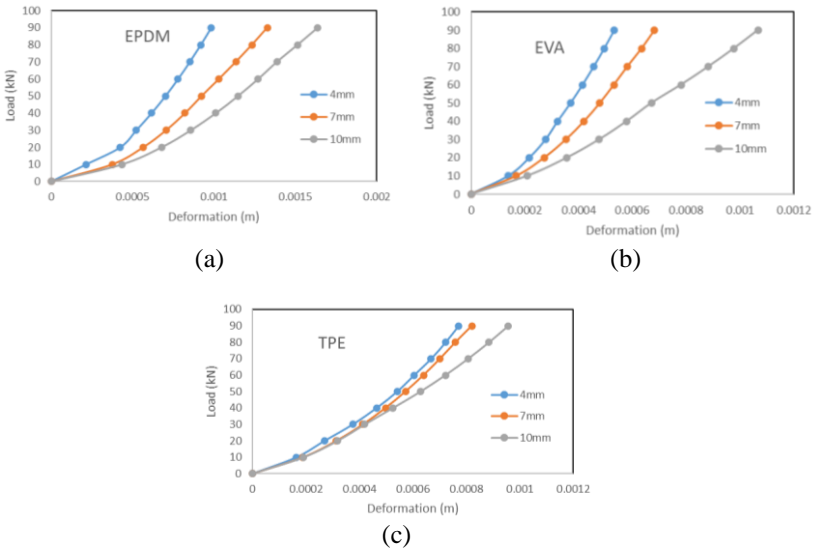
Figure 5: The deformation graph of three similar types of material rail pads under various thicknesses and loads

Rail pads static stiffness

Figure 6 shows the static stiffness for three types of materials with different thicknesses. The static stiffness (k_{st}) is the ratio between the load range (F) and the displacement (δ) range during the last load ramp. It can be calculated using the formula:

$$k_{st} = \frac{F_{final} - F_{initial}}{\delta_{final} - \delta_{initial}} \qquad (2)$$

The results show that the rail pad becomes stiffer as thickness reduces. This is in agreement with previous research [3]. The effect became noticeable when the thickness was less than 6 mm. Thus, the thickness of the rail pads has a significant influence on the mechanical performance under compression pressures induced by rolling trains.

Furthermore, the stiffening conditions on all three rail pads were different. The EPDM pad showed a necessary stiffening above 20 kN. The EVA rail pad was the least stiff. The behaviour of the TPE pad was midway between EPDM and EVA pads, with slight stiffening. These findings were consistent with previous findings [18]. This shows that the rail pads have a wide variety of stiffness values, allowing the choosing of the most appropriate thickness subjected to the design of the railway system and the stresses produced.

The implementation of thin (4 mm) rail pads could be used to decrease the rate of deflections produced by the passage train. However, in real cases, the implementation of low thickness of rail pads may cause extremely stiff tracks. The high stiffness of the rail pad adds to the stiffness due to the configuration of the ballast and formation layers as well as the concrete sleepers. Thus, the greater thickness of rail pads will provide more flexibility and can withstand the higher damping loads [3].

Reaction force on Baseplate

Figure 7 shows the force reaction at the base plate for a load of 90 kN in one second. The results compare the capability of the rail pad to attenuate the static load applied when transferring to the base plate. The higher reaction forces will reduce the life cycle of the baseplate itself. Three types of rail pad materials EPDM, TPE and EVA were tested with the thickness of 5 mm and 10 mm. The results indicated that the reaction force increases with time. Overall, the reaction force was low at the higher thickness of rail pad. EVA showed the highest difference of reaction force with 15% reduction as the thickness of the rail pad increased from 5 mm to 10 mm, while for TPE and EPDM, the reduction was 9% and 5% respectively. It could be seen that the reaction force for EVA was less compared to EPDM and TPE. This showed that the EVA pad had the highest capability to reduce the reaction force at the baseplate compared to EPDM and TPE.
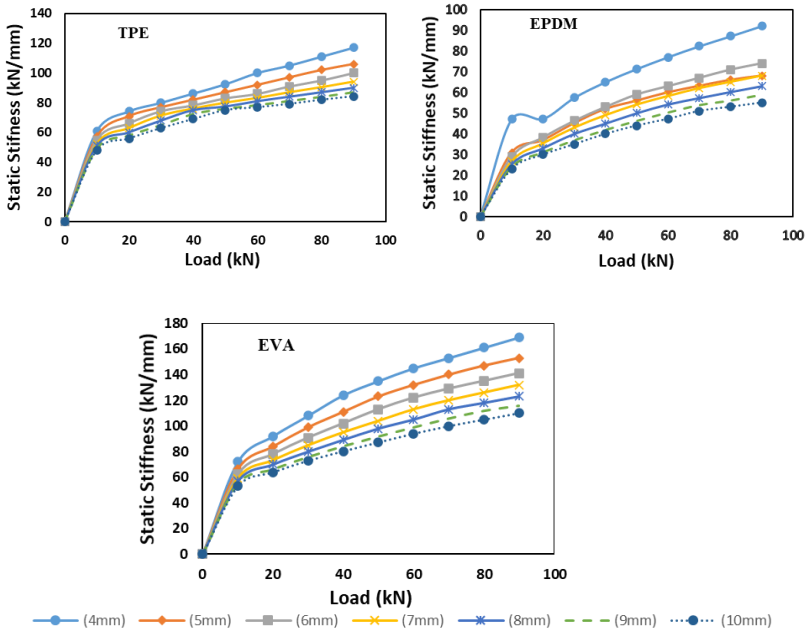
Figure 6: The static stiffness graph for three different materials

The different values of reaction force for different materials and thicknesses were the result of a viscoelastic deformation that occurred due to impact onto the rail-pad [22]. Any such wave will scatter or dampen out over time since the rail pad is viscoelastic and not solely elastic. For thick rail pad the viscoelastic effect was high. This condition increased the time for the energy to dissipate or to dampen that resulting low force transferred to the base plate. The implementation of higher thickness of rail pad in railway industry would be beneficial by way of providing better protection to sleepers and functioning as a ballast layer from the vibration forces. However, the thicker rail pads can cause high rate of track deflection and high values of dissipated energy. This would contribute to the speedy deterioration of track elements (rail, fastening system, etc.) and an increase in train rolling resistance which could result in higher maintenance and exploitation costs [3].
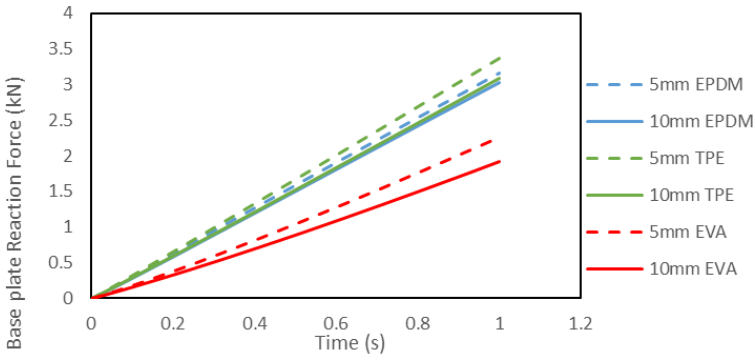
Figure 7: Reaction force of base plate against time tested under different materials of rail pads

Conclusions

The implementation of a baseplate fastening system in railway track will help to mitigate the noise and vibration that are produced from the train vehicle. A fastening system is one of the critical studies for railways so as to know its behaviour under various loads. The presence of a rail pad in a fastening system provides many benefits including the increase of the life cycle of the track which helps to reduce track degradation. The 3D FE model was developed in this study by using ABAQUS software to investigate the behaviour of a baseplate fastening system which focused more on the static analysis. Based on the simulation results, some conclusions can be made throughout this study:

i. The deformation value of a rail pad is influenced by the thickness of the rail pad itself under various loads applied. When thickness is increased, the rail pad has a lower stiffness value which leads to the higher dissipated energy of the railway track system.

ii. The use of different types of rail pads, specifically EPDM, TPE and EVA in track will give significant changes to the track fastening behaviour as the EVA pads have the lowest deformation compared to the other rail pads.

iii. The static stiffness graph shows that the EVA pads give the highest value of stiffness compared to the EPDM and TPE pads. From observation, the classification of rail pads from soft to hard pads can be made by referring to its stiffness. EVA pads are the hardest which are suitable to be used in heavy industry. For the EPDM and TPE pads, they are categorized as soft to medium pads that give benefits to the high-speed track to reduce the track deflection.

    iv.   The baseplate reaction force is influenced by the thickness and types of rail pad used.

Improvement can be made and implemented in this research by executing the dynamic analysis and carrying out experiments for validation purposes. The experiments will also show realistic scenarios to specifically know the behaviour of railway tracks. Other improvements can be made by critically studying the longevity of the base plate fastening system in static and dynamic analysis so as to enable the researcher to predict suitable times to carry out maintenance; hence, reducing the maintenance cost and time. This 3D model could help in making better decisions earlier in order to carry out further track improvement.

Acknowledgement

References

[1]   Z. Zhang, B. Andrawes, and R. E. J, "Parametric Study on the Distribution of Longitudinal Load in Railway Track under Dynamic Wheel Loading Using Finite Element Analysis," *Int. J. Civ. Eng.*, vol. 2, no. 5, pp. 13–27, 2015, doi: 10.14445/23488352/ijce-v2i5p106.

[2]   Getzner Rail Pad, "Rail Pads," no. RT/CE/S/052, pp. 1–2, 1996.

[3]   M. Sol-Sánchez, F. Moreno-Navarro, and M. C. Rubio-Gámez, "The use of deconstructed tire rail pads in railroad tracks: Impact of pad thickness," *Mater. Des.*, vol. 58, pp. 198–203, 2014, doi: 10.1016/j.matdes.2014.01.062.

[4]   K. Knothe, M. Yu, and H. Ilias, "Measurement and Modelling of Resilient Rubber Rail-Pads," *Syst. Dyn. Long-Term Behav. Railw. Veh. Track Subgrade*, pp. 265–274, 2003, doi: 10.1007/978-3-540-45476-2_16.

[5]   M. Sol-Sánchez, F. Moreno-Navarro, and M. C. Rubio-Gámez, "The use of elastic elements in railway tracks: A state of the art review," *Constr. Build. Mater.*, vol. 75, pp. 293–305, 2015, doi: 10.1016/j.conbuildmat.2014.11.027.

[6]   J. Y. Choi, K. Y. Lee, J. S. Chung, and S. H. Kim, "Rail pad corrosion effects on the dynamic behavior of direct fixation track systems in marine environments," *Appl. Sci.*, vol. 10, no. 7, 2020, doi:

10.3390/app10072245.

[7] Y. Tong, G. Liu, K. Yousefian, and G. Jing, "Track Vertical Stiffness – Value, Measurement Methods, Effective Parameters and Challenges: A review," *Transp. Geotech.*, vol. 37, no. December 2021, p. 100833, 2022, doi: 10.1016/j.trgeo.2022.100833.

[8] N. Karpuschenko, D. Velichko, and A. Sevostyanov, "Effectiveness of Intermediate Rail Fastenings on the Railway Sections of Siberia," *Transp. Res. Procedia*, vol. 54, no. 2020, pp. 173–181, 2021, doi: 10.1016/j.trpro.2021.02.062.

[9] K. Wei, P. Zhang, P. Wang, J. Xiao, and Z. Luo, "The influence of amplitude- and frequency-dependent stiffness of rail pads on the random vibration of a vehicle-track coupled system," *Shock Vib.*, vol. 2016, 2016, doi: 10.1155/2016/7674124.

[10] K. Wei, Q. Yang, Y. Dou, F. Wang, and P. Wang, "Experimental investigation into temperature- and frequency-dependent dynamic properties of high-speed rail pads," *Constr. Build. Mater.*, vol. 151, no. October 2018, pp. 848–858, 2017, doi: 10.1016/j.conbuildmat.2017.06.044.

[11] S. Zhu, C. Cai, and P. D. Spanos, "A nonlinear and fractional derivative viscoelastic model for rail pads in the dynamic analysis of coupled vehicle – slab track systems," vol. 335, pp. 304–320, 2015.

[12] M. I. H. Othman, A. M. A. Wahab, M. S. Hadi, and N. M. Noor, "Assessing the nonlinear static stiffness of rail pad using finite element method," *J. Vibroengineering*, vol. 24, no. 5, pp. 921–935, 2022, doi: 10.21595/jve.2022.22293.

[13] S. G. Koroma, M. F. M. Hussein, and J. S. Owen, "Influence of preload and nonlinearity of railpads on vibration of railway tracks under stationary and moving harmonic loads," *J. Low Freq. Noise Vib. Act. Control*, vol. 34, no. 3, pp. 289–306, 2015, doi: 10.1260/0263-0923.34.3.289.

[14] J. Sadeghi, M. Seyedkazemi, and A. Khajehdezfuly, "Nonlinear simulation of vertical behavior of railway fastening system," *Eng. Struct.*, vol. 209, no. September 2019, p. 110340, 2020, doi: 10.1016/j.engstruct.2020.110340.

[15] Z. Chen, M. Shin, S. Wei, B. Andrawes, and D. A. Kuchma, "Finite element modeling and validation of the fastening systems and concrete sleepers used in North America," in *Proceedings of the Institution of Mechanical Engineers, Part F: Journal of Rail and Rapid Transit*, 2014, vol. 228, no. 6, pp. 590–602, doi: 10.1177/0954409714529558.

[16] X. Gao, A. Wang, Y. He, and X. Gu, "Structural Improvement of the ω-Type High-Speed Rail Clip Based on a Study of Its Failure Mechanism," *Shock Vib.*, vol. 2019, 2019, doi: 10.1155/2019/4127065.

[17] T. Bandula-Heva and M. Dhanasekar, "Failure of discontinuous railhead edges due to plastic strain accumulation," *Eng. Fail. Anal.*, vol. 44, no. April, pp. 110–124, 2014, doi: 10.1016/j.engfailanal.2014.04.017.

[18] J. A. Sainz-Aja, I. A. Carrascal, D. Ferreño, J. Pombo, J. A. Casado, and S. Diego, "Influence of the operational conditions on static and dynamic stiffness of rail pads," *Mech. Mater.*, vol. 148, no. June, 2020, doi: 10.1016/j.mechmat.2020.103505.

[19] F. Nishino, S. Malla, and T. Sakurai, "Solution of Finite-Displacement Small-Strain Elasticity Problems by Removal of Rigid Body Displacements," *Doboku Gakkai Ronbunshu*, vol. 2000, no. 661, pp. 11–26, Oct. 2000, doi: 10.2208/jscej.2000.661_11.

[20] M. Amjadi and A. Fatemi, "Tensile behavior of high-density polyethylene including the effects of processing technique, thickness, temperature, and strain rate," *Polymers (Basel).*, vol. 12, no. 9, 2020, doi: 10.3390/POLYM12091857.

[21] S. Bastida, J. I. Eguiazábal, M. Gaztelumendi, and J. Nazábal, "On the thickness dependence of the modulus of elasticity of polymers," *Polym. Test.*, vol. 17, no. 2, pp. 139–145, Apr. 1998, doi: 10.1016/S0142-9418(97)00042-1.

[22] R. L. & C. A. S. Goyal, "Modelling Impact Forces in Elastomers," vol. 22, no. 1, 1999, doi: DOI 10.2495/CMEM990141.